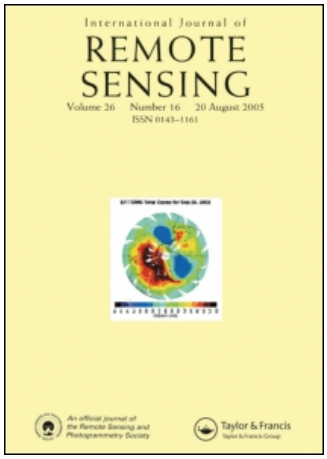

International Journal of Remote Sensing
Publication details, including instructions for authors and subscription information:
http://www.informaworld.com/smpp/title~content=t713722504

Comparison between several feature extraction/classification methods for mapping complicated agricultural land use patches using airborne hyperspectral data

S. Lu [a]; K. Oki [a]; Y. Shimizu [a]; K. Omasa [a]
[a] Graduate School of Agricultural and Life Sciences, The University of Tokyo, Tokyo 113-8657, Japan

Online Publication Date: 01 January 2007
To cite this Article: Lu, S., Oki, K., Shimizu, Y. and Omasa, K. (2007) 'Comparison between several feature extraction/classification methods for mapping complicated agricultural land use patches using airborne hyperspectral data', International Journal of Remote Sensing, 28:5, 963 - 984
To link to this article: DOI: 10.1080/01431160600771561
URL: http://dx.doi.org/10.1080/01431160600771561

International Journal of Remote Sensing
Vol. 28, No. 5, 10 March 2007, 963–984

Taylor & Francis
Taylor & Francis Group

Comparison between several feature extraction/classification methods for mapping complicated agricultural land use patches using airborne hyperspectral data

S. LU, K. OKI, Y. SHIMIZU and K. OMASA*
Graduate School of Agricultural and Life Sciences, The University of Tokyo, 1-1-1 Yayoi, Bunkyo-ku, Tokyo 113-8657, Japan

(*Received 12 July 2005; in final form 19 April 2006*)

Airborne hyperspectral remote sensing was applied to agricultural land in the Miura Peninsula, near the metropolis of Tokyo in Japan. The study area is characterized by complicated land use patches, which is the general characteristic of most agricultural lands in Japan. Several feature extraction/classification methods were examined in classifying the land use and plant species. The results showed that decision boundary feature extraction (DBFE) was better than principal component analysis (PCA) as the feature extraction method. Moreover, the pre-classification process using NDVI that separates the whole study area into vegetated area and non-vegetated areas also improved the classification accuracy. After the pre-procedures, the land use and plant species were finally mapped by maximum likelihood classification (MLC) or extraction and classification of homogeneous objects (ECHO). The best kappa (overall accuracy) of classification was 0.914 (92.4%) and 0.924 (93.3%) for MLC and ECHO, respectively. The best accuracies of each category for the image were 79.5% to 100% for plant species (watermelon, pumpkin, marigold, grass and tree), 88.7% to 100% for soil types, 97.8% for concrete, and 99.4% for vinyl-mulches. Although, built-up area has low estimation accuracy, this did not affect the overall classification accuracy because it covers only a very small area.

1. Introduction

Accurate estimation of agricultural resources that include various types of crops and soils is one of most important tasks in ecological agricultural management. The analysis of remotely sensed data based on spectral differentiation of agricultural surfaces has been developed for the estimation of agricultural resources because it is more cost and time-effective than the conventional field investigation (Dehaan and Taylor 2003). Moreover, the development and the increasing use of airborne imaging spectrometers with high spectral and spatial resolutions have raised the expectation that greater discrimination of vegetation species can be obtained than that of what has been achieved with broad-band sensors in the past (Lewis 2001). The ability of hyperspectral data to discriminate almost similar surfaces even in crop species level offers a good potential to use it as a tool for precision agriculture.

*Corresponding author. Email: aomasa@mail.ecc.u-tokyo.ac.jp

International Journal of Remote Sensing
ISSN 0143-1161 print/ISSN 1366-5901 online
http://www.tandf.co.uk/journals
DOI: 10.1080/01431160600771561

Some hyperspectral data classification efforts have been carried out for discriminating different land cover types such as wetlands (Kumar *et al*. 2001), urban area (Jackson and Landgrebe 2002) and agricultural area (Ortiz *et al.* 1997, Kneubuehler *et al.* 1998, Jimenez *et al.* 1999, Bannari *et al.* 2003). However, thus far, only very few studies have investigated the potential of hyperspectral image for characterization of such complicated agricultural surfaces such as Japanese agricultural land (Oki *et al.* in press). Japanese agricultural lands are characterized by complicated class components and patterns, and usually divided into many various patches planted with different kinds of crops. The farm buildings, roads, vinyl-mulches and different types of soils intensify the complication of the landscape, which makes it more difficult to classify the agricultural lands. In addition, it is often hard to find large enough numbers of training samples to satisfy the requirements of the conventional statistical classification because the areas of the patches of cultivated fields are commonly small.

The objective of this study is to find a feasible classification method for the Japanese agricultural lands. To reduce the dependency of classifiers on a large amount of training samples, the hyperspectral imagery was processed by feature extractions prior to classification. Furthermore, in order to avoid the inter-effect between the man-made land covers and the green covers, we also tried to pre-classify the whole image into vegetated and non-vegetated areas by normalized difference vegetation index (NDVI) before feature extraction was conducted.

2. Study area and data

2.1 *Study area*

The Miura peninsula is located in the south of Tokyo Bay and near the metropolis of Tokyo. Its climate is relatively warm with an oceanic characteristic. The mean annual temperature is 15.4°C and the annual precipitation is about 1530 mm. The peninsula is famous for its radish and cabbage in winter and watermelon in summer. Sometimes grass such as marigold is planted to improve the soil condition during the separation of two seasons for vegetables production. The soil that can be found in the area basically consisted of ando and light ando soil, which are of volcanic origin. Some places show the mixture of ando and light ando soil. The landscape in Miura Peninsula also includes man-made facilities such as concrete roads and built up areas. Some patches of agricultural land are covered with vinyl-mulches. The study area was part of Miura Peninsula (see figure 1), in which most of the above characteristics of land cover were involved.

2.2 *Hyperspectral data and ground truth survey*

AISA (airborne imaging spectroradiometer for application) is an airborne hyperspectral system developed by Specim and is composed of the hyperspectral sensor head, data acquisition computer and miniature GPS/INS sensor. In addition to the sensor systems, Specim provides software, CaliGeo, for radiometric calibration and geo-rectification of hyperspectral data. AISA imagery has a width of 1000 pixels per scan line and it provides wide view in one swath.

The image used in this study was acquired in 21 July 2002 by AISA hyperspectral sensor with 29.9° swath angle. The scanner is carried by an aeroplane, which flew from south to north and records equally at all points across the swath. The data has 70 contiguous spectral bands with wavelength ranging from 400 to 970 nm. The

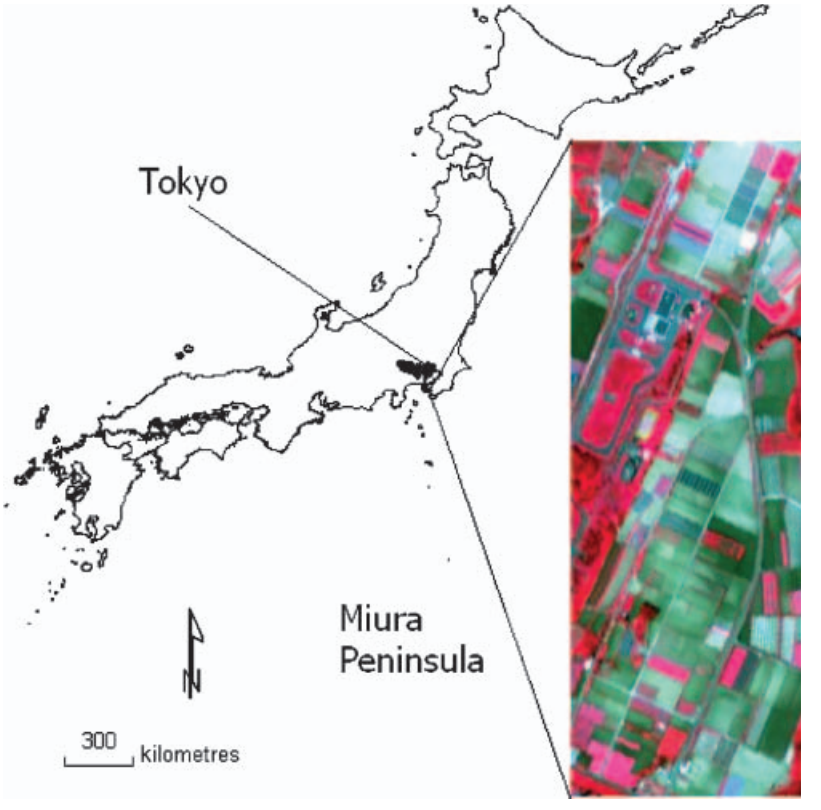

Figure 1. Location map of the study area.

pixel ground resolution is about 2 m × 2 m. The values of the pixel data are 10 000 times of land surface reflectance which has been radiometrically calibrated by the FODIS sensor. The data is quantized as 16-bit.

Training sites for each class were determined by ground truth survey. The ground truth data were divided into training and test data sets. The location of training and test areas are shown in figure 2. The output classes for the vegetated region were watermelon, pumpkin, marigold, maize, grass and tree. Non-vegetated classes were identified as ando soil, light ando soil, mixture of ando soil and light ando soil, built-up, vinyl-mulches and concrete. In addition, since we found only a small number of maize samples during the ground investigation, all of them were used as training samples; hence there were no test samples used to investigate the performance for maize category.

Although different land covers can be delineated from the false colour composite image of the study area, detailed classification is still difficult to perform. The differences in the continuous spectral signatures are expected to be helpful in the classification. Figure 3 shows the spectral signatures of the different classes. The vegetated classes and non-vegetated classes are easily discriminated due to the sharp difference of shapes. But the discrimination within the vegetated and non-vegetated classes was difficult. Hence, some feature extraction methods were used to find the minute differences within the vegetated area and non-vegetated area.

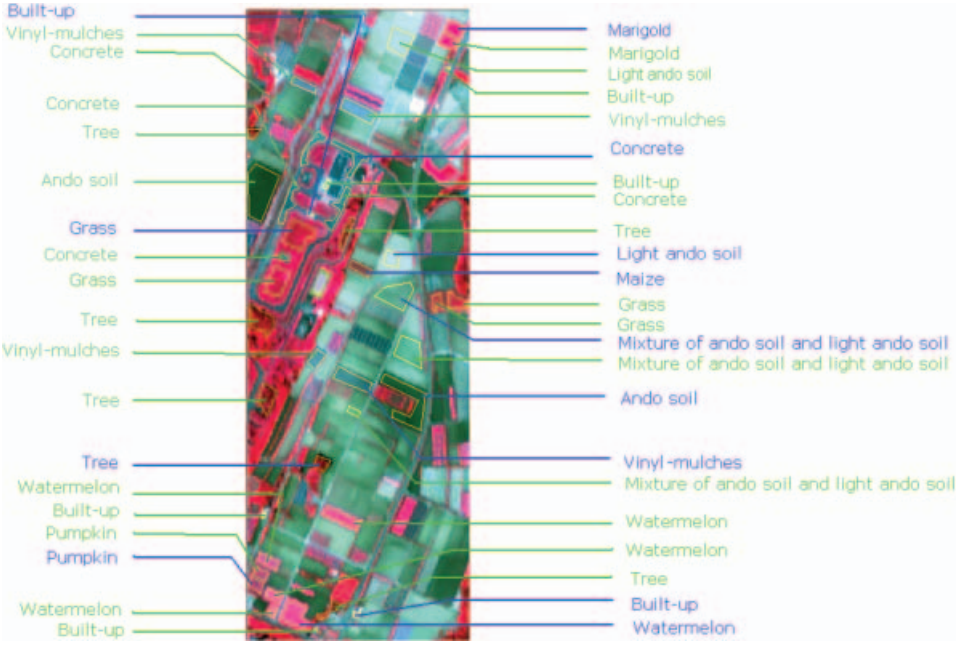

Figure 2. Location map of training and test areas (the green colour represents the training sites, and the blue colour represents test sites).

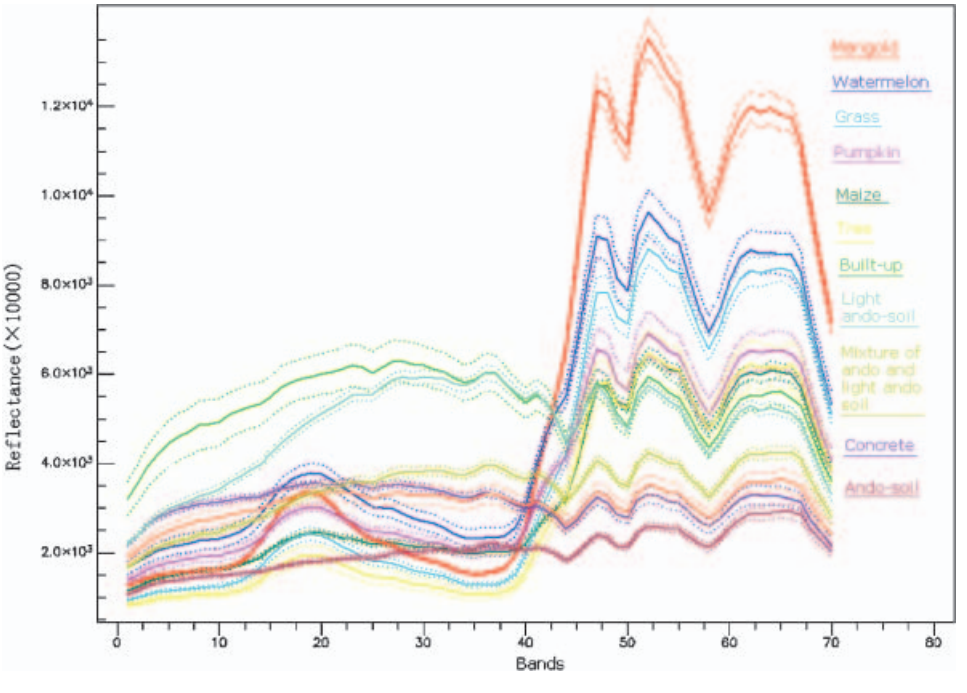

Figure 3. Spectral signature of different classes. The solid lines are the mean spectra of the classes, and the dotted lines are the standard deviations of each class.

3. Analysis of AISA data

The procedure of analysis using the AISA data is illustrated in figure 4. Two feature extraction methods were applied to the original hyperspectral data. The results of PCA or DBFE were inputted to the Maximum Likelihood Classification (MLC) or Extraction and Classification of Homogenous Objects (ECHO) (Kettig and Landgrebe 1976) classifiers. The above procedures produced four feature extraction/classification methods, i.e. PCA-MLC, PCA-ECHO, DBFE-MLC and DBFE-ECHO. The land cover was mapped using the four methods, and the evaluation was carried out to find the best classification method for discriminating the agricultural lands of the Miura Peninsula. All of the feature extractions and classifications were processed by Multispec, developed by David Landgrebe and Larry Biehl at the School of Electrical and Computer Engineering, Purdue University.

The original data were also pre-classified using NDVI into vegetated and non-vegetated images by applying a threshold of 0.3. The objective was to see if there would be an effect in the classification accuracy. The four classification methods were then successively applied into the separated images. The resulting land cover maps of the vegetated and non-vegetated areas were then composed to generate the land cover map of the whole study area. The classification accuracies obtained from these procedures were compared with those without pre-classification procedure.

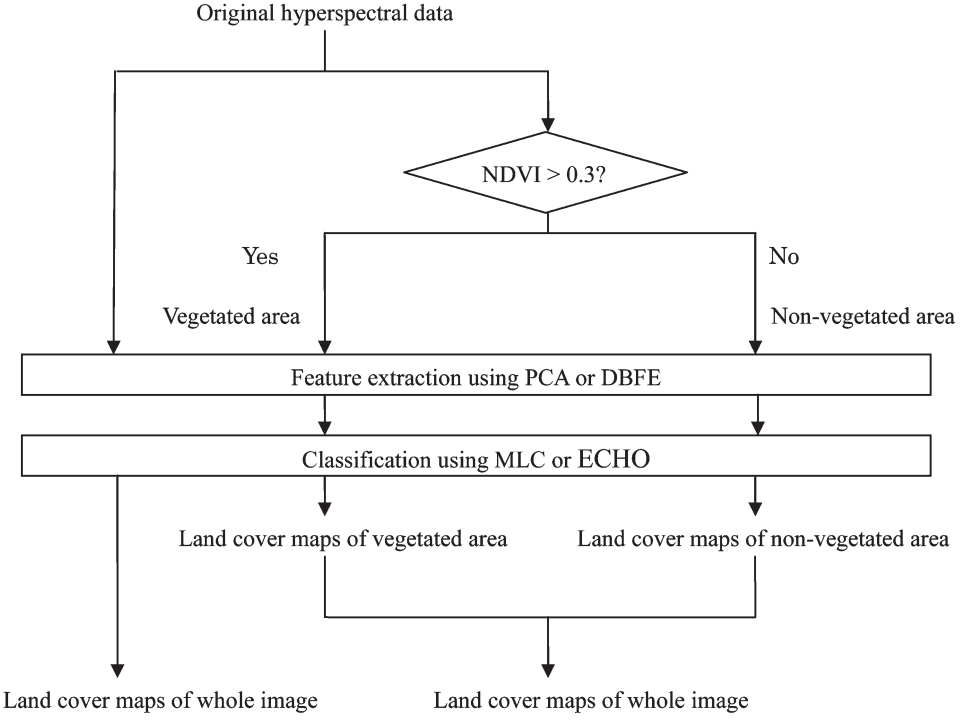

Figure 4. Flowchart of study procedure for agricultural land cover mapping. PCA, principal component analysis; DBFE, decision boundary feature extraction; MLC, maximum likelihood classification; ECHO, extraction and classification of homogeneous objects; NDVI, normalized difference vegetation index.

3.1 *Feature extraction methods*

The availability of a large number of spectral features in hyperspectral data should make it possible to discriminate more ground cover classes with greater accuracy than would be possible using the data from earlier multispectral sensors. Unfortunately, many of the available bands of hyperspectral data are highly correlated and provide redundant information as most of the land surface shared similar spectral characteristics in continuous bands. Furthermore, when the dimensionality of data and the complexity of the decision rule increase, the Hughes effect become more serious (Shahshahani and Landgrebe 1994) and degrade the performance of classification. Thus, in order to realize the potential of the high dimensional data, it is desirable to select the optimum subset of channels for analysis to avoid the Hughes phenomena and parameter estimation problems, as well as to reduce computational requirements.

3.1.1 Principal components analysis (PCA). PCA is normally applied to reduce the dimensionality in the data, and compress as much as possible the information in the original bands into fewer bands. The 'new' bands that result from this statistical procedure are called components. This process relies on the fact that most of the variance in the image can be represented by the first few components. We can then project the original image pixel vectors along with those few eigenvectors, reducing the image dimensionality while retaining the vast majority of the image information. The first three components with accumulative eigenvalues of more than 99% were used in this study for three of the images we classified (the original images, the vegetated area images and non-vegetated area images after pre-classification).

3.1.2 Decision boundary feature extraction (DBFE). Lee and Landgrebe (1993) proposed a method for feature extraction based on decision boundaries for the Bayesian based classifier. In this method, a classifier is first learned for a two-class problem in the input space. The input space for a hyperspectral data is an ordered vector of real number of spectral bands.

Decision boundary is a locus of points in which *a posteriori* probabilities are the same according to Bayes Rule. To prevent deviation of false decision boundary, the process first eliminates the outliers for each class by chi-square threshold. Secondly, a chi-square threshold test of the second class using the mean and covariance of the first class is applied to retain the samples of the second class near to the samples of the first class. The third step is to find the nearest sample of the first class to the sample of the second class retained in the second step. Fourth, find the point where the straight line connecting the pair of samples found in the third step meets the decision boundary. Fifth, find the unit normal vector to the decision boundary at the point found in the fourth step. By repeating the third step to the fifth step, for every point belonging to the first class, the normal vectors with the number same as the points in that class will be calculated. Then, an effective decision boundary feature matrix from the first class of the pair will be estimated. Correspondingly, the effective decision boundary feature matrices of the second class of the pair will be calculated. The sum of the two matrices will be calculated as the estimate of the final effective decision boundary feature matrix. Eigenvectors of the decision boundary feature matrix yield the direction of projection for the two-class problem. The C-class problem where C is the number of the classes is then solved using a sum of the decision boundary feature matrices.

In the study of Lee and Landgrebe (1993) the selection of the optimum features is suggested. The eigenvalues can be added until the accumulation of the eigenvalues

exceeds 95% of the total sum, and the number of the eigenvalues can be set as the rank of the decision boundary feature matrix. To get higher accuracy, 20 features with accumulative eigenvalues of more than 97% were selected for the whole area image, and 15 features with accumulative eigenvalues around 100% were selected for both the separated vegetated and non-vegetated images. The parameters used in the feature extraction process were the default values in the software of MultiSpec.

3.2 *Classification method*

3.2.1 Maximum likelihood classification (MLC). MLC is one of the most commonly used image classification algorithms. The classifier relies on the statistics of a Gaussian probability density function model for each class. When n is the number of bands, X is the image data of n bands, $L_k(X)$ which is the likelihood of X belonging to class k is given by,

$$L_k(\mathbf{X}) = \frac{1}{(2\pi)^{\frac{n}{2}}\left|\sum_k\right|^{\frac{1}{2}}}\exp\left\{-\frac{1}{2}(\mathbf{X}-\boldsymbol{\mu}_k)\sum_k^{-1}(\mathbf{X}-\boldsymbol{\mu}_k)^t\right\}$$

where μ_k is the mean vector of class k; $\sum_k$, the variance-covariance matrix of class k; $|\sum_k|$, the determinant of $\sum_k$.

The pixel is assigned to the class with the highest probability. In the case where the variance-covariance matrix of all classes are equal each other, the MLC is the same as the minimum distance classifier using Euclidian distance, while in the case where the determinants are equal each other, the MLC become the same as the minimum distance classifier using Mahalanobis distances. MLC considers not only the mean, or average values in assigning classification but also the variability of brightness values in each class.

3.2.2 Extraction and classification of homogeneous objects (ECHO). ECHO is a spatial-spectral classifier, i.e. one that incorporates not only spectral variations but spatial ones as well into the decision-making process (Kettig and Landgrebe 1976). ECHO classifies a digital image into fields of spectrally similar pixels before the pixels are assigned to categories. Classification is then conducted using the fields, rather than individual pixels, as the features to be classified (Campbell 1990).

The algorithm first divides the image into small groups consisting of four pixels. For each group, the members are tested for homogeneity by a distance to the centre of the average value of the group. The value of 2%, which represents the portion of the tail of the Gaussian density function, was used to reject the groups, which are not homogenous. Second, an individual group is compared to an adjacent 'field', which is simply a group of one or more connected groups that have previously been merged. If the two samples appear statistically similar by some appropriate criterion, then they too are merged. Otherwise the cell is compared to another adjacent field or becomes a new field itself (Kettig and Landgrebe 1976). For the classification step, a maximum likelihood classifier was applied based on the fields resulted from the scene segmentation process.

3.3 *Separating the whole image into vegetated and non-vegetated area by NDVI*

Hyperspectral data not only give general information of land classes such as the vegetation and soil, but also provide more details in the species of vegetation or soil types. When we aimed to distinguish the species of crops or types of soils in a

single-step without the NDVI procedure, the little difference between the subclasses seems to be obscured by the difference between the main classes such as vegetated and non-vegetated regions. Thus, we separated the vegetated regions from non-vegetated regions using NDVI, which reflects living biomass in each pixel. The NDVI value was computed using the band 35 (683 nm) and band 47 (783 nm) representing red and near-infrared band. This procedure was expected to prevent confusion among categories in classification process. The pixels with the NDVI value larger than 0.3 was assigned as vegetated pixels, while pixels smaller than 0.3 was defined as non-vegetated pixels. This threshold value showed that vegetated areas and non-vegetated areas can be accurately delineated as validated by collected ground information. The subclasses were then discriminated within the separated vegetated image and non-vegetated image by the above feature extraction/classification methods.

4. Results and discussion

4.1 *Classification for the whole image without pre-classification by NDVI*

The confusion matrices for the four methods without pre-classification by NDVI are listed in table 1. The accuracy and kappa statistics on the test data sets are shown in table 2, while the classification result is shown in figure 5. The overall accuracy is defined as the overall proportion of correctly classified pixels in the sample used to construct the confusion matrix. The correct number is the sum of the diagonal entries. Dividing this value by the total number of pixels examined gives the proportion that has been correctly classified. Kappa statistic is an index, which compares the agreement against that which might be expected by chance. Kappa can be thought of as the chance-corrected proportional agreement, and possible values range from $+1$ (perfect agreement) via 0 (no agreement above that expected by chance) to -1 (complete disagreement). In view of both kappa statistic and overall accuracy, the classification without separating by NDVI results to the following: DBFE-ECHO and DBFE-MLC, PCA-ECHO and PCA-MLC ranked from best to worst. For the same classifier, the DBFE input showed a better result than PCA. On the other hand, in the PCA inputs, ECHO presented little difference with MLC.

The classification accuracy of DBFE input was much better than PCA in watermelon, grass, mixture of ando and light ando soil, concrete and vinyl mulches, with an exception for built-up areas. The low estimation accuracy for built-up areas is probably due to the diverse materials of different buildings. However, this did not affect the performance of classification because the built-up category only covers a very small area. Since both ECHO and MLC classifiers performed well using the DBFE data as inputs, it was assumed that the transformation of DBFE can be used successfully for the classification of hyperspectral imagery. ECHO and MLC classifiers using the DBFE input performed the same with 0.832 (85.0%) kappa (overall accuracy). But some improvement should be made for the estimation of tree and the class of mixture of ando and light ando soil. Considering the performance of classifiers, although the DBFE inputs had the same results by each classifier, ECHO which considered the contexture yielded slightly better results for the entire data set than the pixel-based MLC using the same PCA input.

4.2 *Classification with pre-classification by NDVI*

In order to improve the discrimination of some categories such as tree or mixture of ando and light ando soil which were poorly estimated in the previous method, we

Table 1. Confusion matrices for four methods without pre-classification by NDVI. The left-hand side (*y* axis) is labelled with the categories on the verification sites; the upper edge (*x* axis) is labelled with the same categories; these refer to those on the verification sites to be evaluated. The class of 'mixture soil' in the confusion matrix is the class of 'mixture of ando and light ando soil' and the 'light-ando' is the class of light ando soil.

(a) The confusion matrix for PCA-MLC.

			Number	0	1	2	3	4	5	6	7	8	9	10	11	12
Class name	Class number	Accuracy* (%)	Samples	Background	Mixture soil	Ando-soil	Built-up	Concrete	Vinyl-mulches	Light-ando	Grass	Marigold	Maize	Tree	Watermelon	Pumpkin
Mixture soil	1	9.5	399	0	38	0	346	0	15	0	0	0	0	0	0	0
Ando-soil	2	100	329	0	0	329	0	0	0	0	0	0	0	0	0	0
Built-up	3	80.6	36	5	0	0	29	0	2	0	0	0	0	0	0	0
Concrete	4	75.7	313	0	0	0	0	237	70	0	0	0	6	0	0	0
Vinyl mulches	5	34.6	315	0	0	0	23	183	109	0	0	0	0	0	0	0
Light-ando	6	100	144	0	0	0	0	0	0	144	0	0	0	0	0	0
Grass	7	87.1	443	0	0	0	0	0	0	0	386	5	0	0	23	29
Marigold	8	97.6	83	0	0	0	0	0	0	0	0	81	0	0	2	0
Maize	9	0	0	0	0	0	0	0	0	0	0	0	0	0	0	0
Tree	10	65.8	503	0	0	0	0	0	0	0	141	0	7	331	0	24
Watermelon	11	66.3	288	0	0	0	0	0	0	0	0	0	0	0	191	97
Pumpkin	12	88.7	71	0	0	0	0	0	0	0	0	0	8	0	0	63
Total			2924	5	38	329	398	420	196	144	527	86	21	331	216	213
reliability accuracy (%)†					100	100	7.3	56.4	55.6	100	73.2	94.2	0	100	88.4	29.6

Overall accuracy (1938/2924)=66.3%.
Kappa statistic=0.626.
*(100, percent omission error) also called producer's accuracy.
†(100, percent commission error) also called user's accuracy.

(b) The confusion matrix for PCA-ECHO.

			Number	0	1	2	3	4	5	6	7	8	9	10	11	12
Class name	Class number	Accuracy* (%)	Samples	Background	Mixture soil	Ando-soil	Built-up	Concrete	Vinyl-mulches	Light-ando	Grass	Marigold	Maize	Tree	Watermelon	Pumpkin
Mixture soil	1	9.5	399	0	38	0	346	0	15	0	0	0	0	0	0	0
Ando-soil	2	100	329	0	0	329	0	0	0	0	0	0	0	0	0	0
Built-up	3	80.6	136	5	0	0	29	0	2	0	0	0	0	0	0	0
Concrete	4	86.3	313	0	0	0	0	270	37	0	0	0	6	0	0	0
Vinyl mulches	5	34.6	315	0	0	0	23	183	109	0	0	0	0	0	0	0
Light-ando	6	100	144	0	0	0	0	0	0	144	0	0	0	0	0	0
Grass	7	86.5	443	0	0	0	0	0	0	0	383	5	4	0	23	28
Marigold	8	97.6	83	0	0	0	0	0	0	0	0	81	0	0	2	0
Maize	9	0	0	0	0	0	0	0	0	0	0	0	0	0	0	0
Tree	10	77.5	503	0	0	0	0	0	0	0	88	0	6	390	0	19
Watermelon	11	66.3	288	0	0	0	0	0	0	0	0	0	0	0	191	97
Pumpkin	12	100	71	0	0	0	0	0	0	0	0	0	0	0	0	71
Total			2924	5	38	329	398	453	163	144	471	86	16	390	216	215
reliability accuracy (%)†					100	100	7.3	59.6	66.9	100	81.3	94.2	0	100	88.4	33

Overall accuracy (2035/2924)=69.6%.
Kappa statistic=0.663.
*(100, percent omission error) also called producer's accuracy.
†(100, percent commission error) also called user's accuracy.

(c) The confusion matrix for DBFE-MLC.

			Number	0	1	2	3	4	5	6	7	8	9	10	11	12
Class name	Class number	Accuracy* (%)	Samples	Background	Mixture soil	Ando-soil	Built-up	Concrete	Vinyl-mulches	Light-ando	Grass	Marigold	Maize	Tree	Watermelon	Pumpkin
Mixture soil	1	51.6	399	0	206	0	192	0	0	1	0	0	0	0	0	0
Ando-soil	2	100	329	0	0	329	0	0	0	0	0	0	0	0	0	0
Built-up	3	33.3	36	12	0	0	12	2	10	0	0	0	0	0	0	0
Concrete	4	95.5	313	0	0	0	1	229	5	0	0	0	4	0	0	4
Vinyl mulches	5	98.4	315	4	0	0	1	0	310	0	0	0	0	0	0	0
Light-ando	6	100	144	0	0	0	0	0	0	144	0	0	0	0	0	0
Grass	7	95.5	443	2	0	0	0	0	0	0	423	0	1	0	4	13
Marigold	8	96.6	83	0	0	0	0	0	0	0	0	80	0	0	3	0
Maize	9	0	0	0	0	0	0	0	0	0	0	0	0	0	0	0
Tree	10	67.2	503	1	0	0	0	0	0	0	84	0	35	338	0	45
Watermelon	11	95.1	288	0	0	0	0	0	0	0	0	0	0	0	274	14
Pumpkin	12	100	71	0	0	0	0	0	0	0	0	0	8	0	0	71
Total			2924	19	206	329	206	301	325	145	507	80	40	338	281	147
reliability accuracy (%)†					100	100	5.8	99.3	95.4	99.3	83.4	100	0	100	97.5	48.3

Overall accuracy (2486/2924)=85.0%.
Kappa statistic=0.832.
*(100, percent omission error) also called producer's accuracy.
†(100, percent commission error) also called user's accuracy.

(d) The confusion matrix for DBFE-ECHO.

Class name	Class number	Accuracy* (%)	Number of samples	0 Background	1 Mixture soil	2 Ando-soil	3 Built-up	4 Concrete	5 Vinyl-mulches	6 Light-ando	7 Grass	8 Marigold	9 Maize	10 Tree	11 Watermelon	12 Pumpkin
Mixture soil	1	51.6	399	0	206	0	192	0	0	1	0	0	0	0	0	0
Ando-soil	2	100	329	0	0	329	0	0	0	0	0	0	0	0	0	0
Built-up	3	33.3	136	12	0	0	12	2	10	0	0	0	0	0	0	0
Concrete	4	95.5	313	0	0	0	1	229	5	0	0	0	4	0	0	4
Vinyl mulches	5	98.4	315	4	0	0	1	0	310	0	0	0	0	0	0	0
Light-ando	6	100	144	0	0	0	0	0	0	144	0	0	0	0	0	0
Grass	7	95.5	443	2	0	0	0	0	0	0	423	0	1	0	4	13
Marigold	8	96.6	83	0	0	0	0	0	0	0	0	80	0	0	3	0
Maize	9	0	0	0	0	0	0	0	0	0	0	0	0	0	0	0
Tree	10	67.2	503	1	0	0	0	0	0	0	84	0	35	338	0	45
Watermelon	11	95.1	288	0	0	0	0	0	0	0	0	0	0	0	274	14
Pumpkin	12	100	71	0	0	0	0	0	0	0	0	0	8	0	0	71
Total			2924	19	206	329	206	301	325	145	507	80	40	338	281	147
reliability accuracy (%)†					100	100	5.8	99.3	95.4	99.3	83.4	100	0	100	97.5	48.3

Overall accuracy (2486/2924)=85.0%.
Kappa statistic=0.832.
*(100, percent omission error) also called producer's accuracy.
†(100, percent commission error) also called user's accuracy.

Table 2. Classification accuracies of agricultural land image unseparated by NDVI.

	Class	Accuracy*			
		PCA-MLC	PCA-ECHO	DBFE-MLC	DBFE-ECHO
Vegetated areas	Watermelon	66.3%	66.3%	95.1%	95.1%
	Pumpkin	88.7	100	100	100
	Marigold	97.6	97.6	96.4	96.4
	Maize	0	0	0	0
	Grass	87.1	86.5	95.5	95.5
	Trees	65.8	77.5	67.2	67.2
	Overall (vegetated)	75.8%	80.4%	85.4%	85.4%
	Kappa statistic (vegetated)	0.724	0.737	0.804	0.804
Non-vegetated areas	Ando-soil	100%	100%	100%	100%
	Light ando soil	100	100	100	100
	Mixture soil	9.5	9.5	51.6	51.6
	Built-up	80.6	80.6	33.3	33.3
	Concrete	75.7	86.3	95.5	95.5
	Vinyl mulches	34.6	34.6	98.4	98.4
	Overall (non-vegetated)	57.7%	59.8%	84.6%	84.6%
	Kappa statistic (non-vegetated)	0.502	0.528	0.812	0.812
Whole image	Overall (whole)	66.3%	69.6%	85.0%	85.0%
	Kappa statistic	0.626	0.663	0.832	0.832

*Each category accuracy is the producer's accuracy

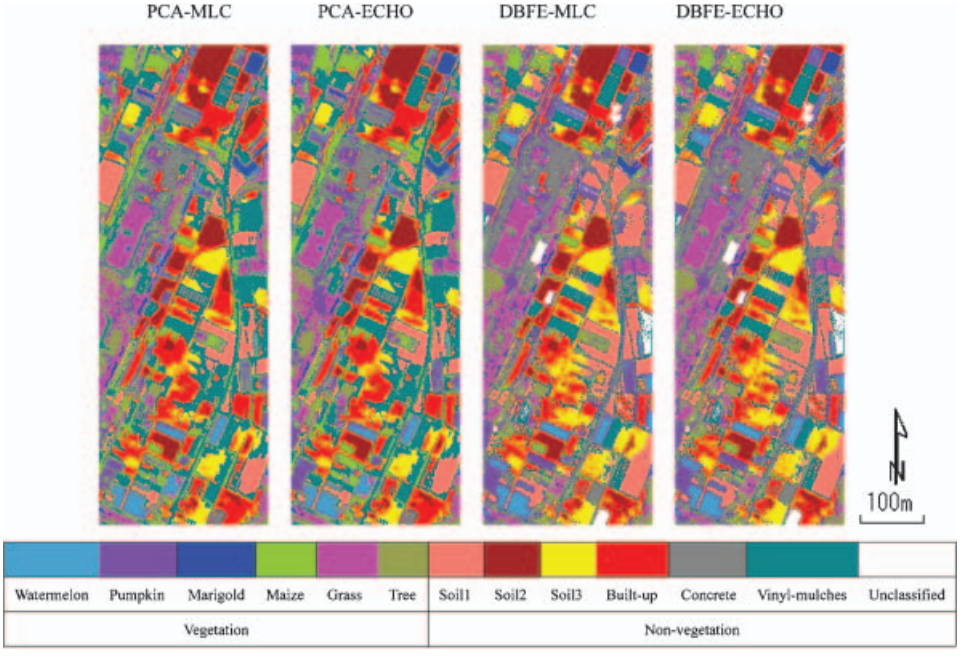

Figure 5. Classification results of agricultural land image without pre-classification by NDVI. Soil1 is the ando-soil, soil2 is the light ando soil and soil3 is the mixture of ando and light ando soil.

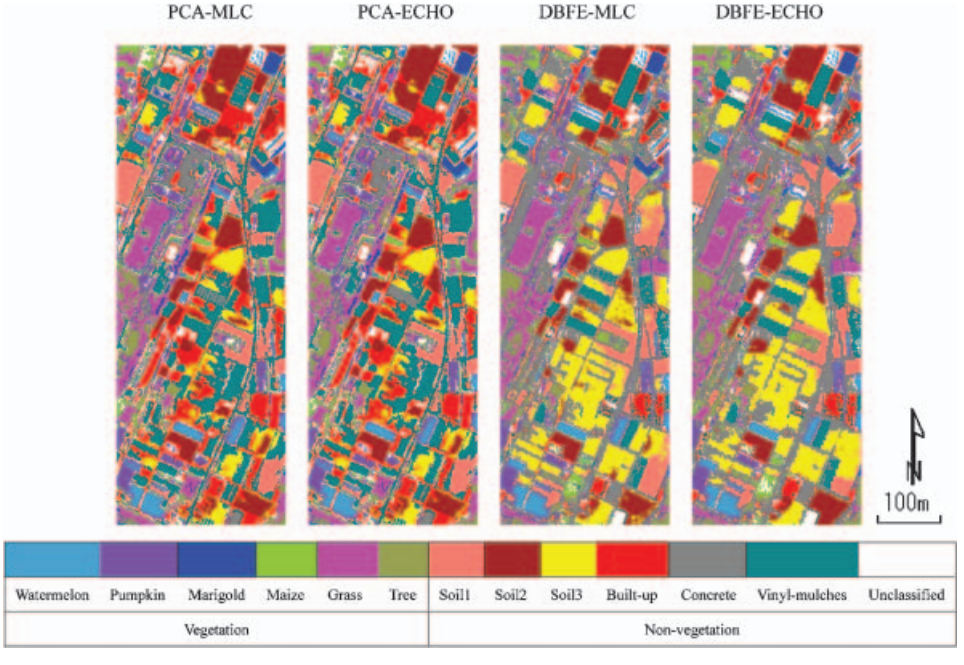

Figure 6. Classification results of agricultural land image with pre-classification by NDVI. Soil1 is the ando-soil, soil2 is the light ando soil and soil3 is the mixture of ando and light ando soil.

tried to pre-classify the image into vegetated area and non-vegetated area by NDVI using a threshold of 0.3, before performing the feature extraction and classification using the four methods. The confusion matrices for the four methods with pre-classification by NDVI are listed in table 3. The accuracy and kappa statistics on the test data sets are shown in table 4, while the classification result is shown in figure 6.

The pre-classification procedure improved the accuracy of each classification method. For example, the PCA-MLC in the single-step classification without pre-classification by NDVI resulted with a kappa (overall accuracy) of 0.626 (66.3%), while the same classification method with NDVI procedure yielded the value of kappa (overall accuracy) approaching 0.694 (72.5%). For the classifier of DBFE-ECHO which performed well in the single-step procedure, the kappa (overall accuracy) also improved from 0.832 (85.0%) to 0.924 (93.3%). The other two methods also obtained higher accuracy compared to that of without pre-classification by NDVI.

The overall accuracy of both vegetated area and non-vegetated area has increased appreciably. For the vegetated area classified by PCA-MLC and PCA-ECHO, the kappa statistic (overall accuracy) increased from 0.724 (75.8%) and 0.737 (80.4%) to 0.784 (84.0%) and 0.783 (83.9%), respectively, compared to the classification without pre-classification by NDVI. The DBFE-MLC and DBFE-ECHO methods yielded 0.856 (89.5%) and 0.878 (91.1%) classification accuracy with 0.052 (4.1%) and 0.074 (5.7%) improvement, respectively.

For the individual category, the four methods performed well for pumpkin, marigold, ando soil and light ando soil. A big improvement was found in identification of mixture of ando and light ando soil class. The best classification accuracy achieved was 88.7% using the DBFE-ECHO method with pre-classification by NDVI. On the other hand, without the pre-classification, the best accuracy was only 51.6%. The tree mapping was also improved from 67.2% to 79.5% by the DBFE-ECHO method. The best producer's accuracies of each category for the image were 79.5% to 100% for plant species (watermelon, pumpkin, marigold, grass and tree), 88.7% to 100% for soil types, 97.8% for concrete, and 99.4% for vinyl mulches.

The results showed that hyperspectral remote sensing data can be applied to characterize complex agricultural lands. Here proper selection of feature extraction methods was very important. DBFE was found to be superior to PCA in classifying agricultural land cover in the present study. The main reason lies on PCA which is based on the whole data statistics, unlike DBFE which based classification directly on the training samples. PCA minimizes the mean square error for a given number of features but in classification it is desirable to extract features which are focused on discriminating between classes. PCA tries to project the data onto a lower dimension that favours discriminating the classes which are having the largest inter-variance (Cheriyadat and Bruce 2003). But when the classes have a small difference in mean value, the information contained in lower dimension may not be appropriate for discriminating them and thus degrading overall classification accuracy. The superiority of DBFE to PCA is that it does not deteriorate even when there is little or no mean difference between classes, because the transformation is based upon not only the mean value difference, but also the covariance between the training samples (Lee and Landgrebe 1993).

The accuracy was also improved after separating the data into vegetated and non-vegetated areas. The result implied that the pre-classification by NDVI prevented the spectral confusion between the classes under the vegetated and non-vegetated areas.

Table 3. Confusion matrices for four methods with pre-classification by NDVI. The left-hand side (*y* axis) is labelled with the categories on the verification sites; the upper edge (*x* axis) is labelled with the same categories; these refer to those on the verification sites to be evaluated. The class of 'mixture soil' in the confusion matrix is the class of 'mixture of ando and light ando soil' and the 'light-ando' is the class of light ando soil.

(a) The confusion matrix for PCA-MLC.

			Number	0	1	2	3	4	5	6	7	8	9	10	11	12
Class name	Class number	Accuracy* (%)	Samples	Background	Mixture soil	Ando-soil	Built-up	Concrete	Vinyl-mulches	Light-ando	Grass	Marigold	Maize	Tree	Watermelon	Pumpkin
Mixture soil	1	8.8	399	0	35	0	220	0	144	0	0	0	0	0	0	0
Ando-soil	2	100	329	0	0	329	0	0	0	0	0	0	0	0	0	0
Built-up	3	75	36	9	0	0	27	0	0	0	0	0	0	0	0	0
Concrete	4	62	313	4	0	0	10	194	105	0	0	0	0	0	0	0
Vinyl mulches	5	71.7	315	0	0	0	88	1	226	0	0	0	0	0	0	0
Light-ando	6	100	144	0	0	0	0	0	0	144	0	0	0	0	0	0
Grass	7	91.2	443	0	0	0	0	0	0	0	404	1	27	0	10	1
Marigold	8	95.2	83	0	0	0	0	0	0	0	0	79	0	0	4	0
Maize	9	0	0	0	0	0	0	0	0	0	0	0	0	0	0	0
Tree	10	70.6	503	0	0	0	0	0	0	0	117	0	19	355	0	12
Watermelon	11	89.2	288	0	0	0	0	0	0	0	0	0	0	0	257	31
Pumpkin	12	100	71	0	0	0	0	0	0	0	0	0	0	0	0	71
Total			2924	13	35	329	345	195	475	144	521	80	46	355	271	115
reliability accuracy (%)†					100	100	7.8	99.5	47.6	100	77.5	98.8	0	100	94.8	61.7

Overall accuracy (2121/2924)=72.5%.
Kappa statistic=0.694.
*(100, percent omission error) also called producer's accuracy.
†(100, percent commission error) also called user's accuracy.

(b) The confusion matrix for PCA-ECHO.

			Number	0	1	2	3	4	5	6	7	8	9	10	11	12
Class name	Class number	Accuracy* (%)	Samples	Background	Mixture soil	Ando-soil	Built-up	Concrete	Vinyl-mulches	Light-ando	Grass	Marigold	Maize	Tree	Watermelon	Pumpkin
Mixture soil	1	8.8	399	0	35	0	220	0	144	0	0	0	0	0	0	0
Ando-soil	2	100	329	0	0	329	0	0	0	0	0	0	0	0	0	0
Built-up	3	75	36	9	0	0	27	0	0	0	0	0	0	0	0	0
Concrete	4	74.1	313	4	0	0	10	232	67	0	0	0	0	0	0	0
Vinyl mulches	5	71.7	315	0	0	0	88	1	226	0	0	0	0	0	0	0
Light-ando	6	100	144	0	0	0	0	0	0	144	0	0	0	0	0	0
Grass	7	91	443	0	0	0	0	0	0	0	403	1	29	0	10	0
Marigold	8	95.2	83	0	0	0	0	0	0	0	0	79	0	0	4	0
Maize	9	0	0	0	0	0	0	0	0	0	0	0	0	0	0	0
Tree	10	70.6	503	0	0	0	0	0	0	0	116	0	20	355	0	12
Watermelon	11	89.2	288	0	0	0	0	0	0	0	0	0	0	0	257	31
Pumpkin	12	100	71	0	0	0	0	0	0	0	0	0	0	0	0	71
Total			2924	13	35	329	345	233	437	144	519	80	49	355	271	114
reliability accuracy (%)†					100	100	7.8	99.6	51.7	100	77.6	98.8	0	100	94.8	62.3

Overall accuracy (2158/2924)=73.8%.
Kappa statistic=0.708.
*(100, percent omission error) also called producer's accuracy.
†(100, percent commission error) also called user's accuracy.

(c) The confusion matrix for DBFE-MLC.

			Number	0	1	2	3	4	5	6	7	8	9	10	11	12
Class name	Class number	Accuracy* (%)	Samples	Background	Mixture soil	Ando-soil	Built-up	Concrete	Vinyl-mulches	Light-ando	Grass	Marigold	Maize	Tree	Watermelon	Pumpkin
Mixture soil	1	88.5	399	0	353	0	0	0	0	46	0	0	0	0	0	0
Ando-soil	2	100	329	0	0	329	0	0	0	0	0	0	0	0	0	0
Built-up	3	47.2	36	15	0	0	17	0	4	0	0	0	0	0	0	0
Concrete	4	97.4	313	2	0	0	5	305	1	0	0	0	0	0	0	0
Vinyl mulches	5	99.4	315	0	0	0	1	1	313	0	0	0	0	0	0	0
Light-ando	6	100	144	0	0	0	0	0	0	144	0	0	0	0	0	0
Grass	7	97.3	443	1	0	0	0	0	0	0	431	0	2	0	0	9
Marigold	8	98.8	83	0	0	0	0	0	0	0	0	82	0	0	1	0
Maize	9	0	0	0	0	0	0	0	0	0	0	0	0	0	0	0
Tree	10	74.8	503	1	0	0	0	0	0	0	103	0	16	376	0	7
Watermelon	11	97.9	288	0	0	0	0	0	0	0	0	0	1	0	282	5
Pumpkin	12	100	71	0	0	0	0	0	0	0	0	0	0	0	0	71
Total			2924	19	353	329	23	306	318	190	534	82	19	376	283	92
reliability accuracy (%)†					100	100	73.9	99.7	98.4	75.8	80.7	100	0	100	99.6	77.2

Overall accuracy (2703/2924)=92.4%.
Kappa statistic=0.914.
*(100, percent omission error) also called producer's accuracy.
†(100, percent commission error) also called user's accuracy.

(d) The confusion matrix for DBFE-ECHO.

			Number	0	1	2	3	4	5	6	7	8	9	10	11	12
Class name	Class number	Accuracy* (%)	Samples	Background	Mixture soil	Ando-soil	Built-up	Concrete	Vinyl-mulches	Light-ando	Grass	Marigold	Maize	Tree	Watermelon	Pumpkin
Mixture soil	1	88.7	399	0	354	0	0	0	0	45	0	0	0	0	0	0
Ando-soil	2	100	329	0	0	329	0	0	0	0	0	0	0	0	0	0
Built-up	3	47.2	36	15	0	0	17	0	4	0	0	0	0	0	0	0
Concrete	4	97.8	313	2	0	0	4	306	1	0	0	0	0	0	0	0
Vinyl mulches	5	99	315	0	0	0	2	1	312	0	0	0	0	0	0	0
Light-ando	6	100	144	0	0	0	0	0	0	144	0	0	0	0	0	0
Grass	7	97.1	443	9	0	0	0	0	0	0	430	0	1	0	0	3
Marigold	8	98.8	83	0	0	0	0	0	0	0	0	82	0	0	1	0
Maize	9	0	0	0	0	0	0	0	0	0	0	0	0	0	0	0
Tree	10	79.5	503	1	0	0	0	0	0	0	85	0	11	400	0	6
Watermelon	11	97.9	288	0	0	0	0	0	0	0	0	0	0	0	282	6
Pumpkin	12	100	71	0	0	0	0	0	0	0	0	0	0	0	0	71
Total			2924	27	354	329	23	307	317	189	515	82	19	400	283	86
reliability accuracy (%)†					100	100	73.9	99.7	98.4	76.2	83.5	100	0	100	99.6	82.6

Overall accuracy (2727/2924)=93.3%.
Kappa statistic=0.924.
*(100, percent omission error) also called producer's accuracy.
†(100, percent commission error) also called user's accuracy.

Table 4. Classification accuracies of agricultural land image separated by NDVI.

		Accuracy*			
	Class	PCA-MLC	PCA-ECHO	DBFE-MLC	DBFE-ECHO
Vegetated area	Watermelon	89.2%	89.2%	97.9%	97.9%
	Pumpkin	100	100	100	100
	Marigold	95.2	95.2	98.8	98.8
	Maize	0	0	0	0
	Grass	91.2	89.2	97.3	97.1
	Tree	70.6	70.6	74.8	79.5
	Overall (vegetated)	84.0%	83.9%	89.5%	91.1%
	Kappa statistic (vegetated)	0.784	0.783	0.856	0.878
Non-vegetated areas	Ando-soil	100%	100%	100%	100%
	Light ando	100	100	100	100
	Mixture soil	8.8	8.8	88.5	88.7
	Built-up	75.0	75.0	47.2	47.2
	Concrete	62.0	74.1	97.4	97.8
	Vinyl mulches	71.7	71.7	99.4	99.0
	Overall (non-vegetated)	62.2%	64.6%	95.1%	95.2%
	Kappa statistic (non-vegetated)	0.552	0.582	0.939	0.940
Whole image	Overall (whole)	72.5%	73.8%	92.4%	93.3%
	Kappa statistic	0.694	0.708	0.914	0.924

*Each category accuracy is the producer's accuracy.

The classification accuracies shown here are obtained by the selected verification areas listed in the figure 2. In general, purely random points may give lower classification accuracies. But since the same verification areas were used for each classification method, it will not change the result of the comparison of the classification methods.

5. Conclusion

This research described an encouraging finding for using hyperspectral imagery to map diverse agricultural land covers near the metropolis of Tokyo. The research has evaluated the different classification methods for processing AISA hyperspectral imagery. Based on the results, DBFE is suited for improving the classification of complex agricultural lands in Japan. This is basically because of its capability of distinguishing between classes based on training samples, thus also reducing the dimensionality of the data.

Moreover, the pre-classification process using NDVI that separate the whole image into vegetated area and non-vegetated area also improved the classification accuracy. This is due to the elimination of spectral confusion between categories. Hence, this study concluded that the combination of pre-classification by NDVI and DBFE method is the most appropriate for classifying the complicated agricultural land use patches in Miura Peninsula.

Acknowledgments

We thank Larry Biehl and David Landgrebe of Purdue University for providing the MultiSpec software online. We also thank Alejandro M. de Asis of Tokyo University for his useful discussions. Thanks also to Tomoyuki Suhama of Center for Geo-Information Technology Integration, PASCO Corporation provided the hyperspectral data for this study. We are especially thankful to the reviewers for their constructive comments and suggestions.

References

BANNARI, A., CHEVERIE, M., STAENZ, K. and MCNAIRN, H., 2003, Senescent vegetation and crop residue mapping in agricultural lands using artificial neutral networks and hyperspectral remote sensing. In *Proceedings of the Geoscience and Remote Sensing Symposium 2003 (IGARSS '03), 2003 IEEE International*, pp. 4292–4294.

CAMPBELL, J.B., 1990, *Introduction to Remote Sensing* (New York, NY: The Guilford Press).

CHERIYADAT, A. and BRUCE, L.M., 2003, Why principal component analysis is not an appropriate feature extraction method for hyperspectral data. *Proceedings of the Geoscience and Remote Sensing Symposium 2003 (IGARSS '03), 2003 IEEE International*, pp. 3420–3422.

DEHAAN, R. and TAYLOR, G.R., 2003, Image-derived spectral endmembers as indicators of salinisation. *International Journal of Remote Sensing*, **24**, pp. 775–794.

JACKSON, Q. and LANDGREBE, D.A., 2002, Adaptive Bayesian contextual classification based on Markov random fields. *IEEE Transactions on Geoscience and Remote Sensing*, **40**, pp. 2454–2463.

JIMENEZ, L.O. and LANDGREBE, D.A., 1999, Hyperspectral data analysis and supervised feature reduction via projection pursuit. *IEEE Transactions on Geoscience and Remote Sensing*, **37**, pp. 2653–2667.

KETTIG, R.L. and LANDGREBE, D.A., 1976, Classification of multispectral image data by extraction and classification of homogeneous objects. *IEEE Transactions on Geoscience Electronics*, **GE-14**, pp. 19–26.

KNEUBUEHLER, M., SCHAEPMAN, M.E. and KELLENBERGER, T.W., 1998, Comparison of different approaches of selecting endmembers to classify agricultural land by means of hyperspectral data (DAIS 7915). In *Proceedings of the Geoscience and Remote Sensing Symposium 1998 (IGARSS '98), 1998 IEEE International*, 6–10 July 1998, Seattle, WA (Piscataway, NJ: IEEE), pp. 888–890.

KUMAR, S., GHOSH, J. and CRAWFORD, M.M., 2001, Best-bases feature extraction algorithms for classification of hyperspectral data. *IEEE Transactions on Geoscience and Remote Sensing*, **39**, pp. 1368–1379.

LANDGREBE, D.A. and BIEHL, L., An introduction to multiSpec Version 5.2001. Available online at: http://www.ece.purdue.edu/~biehl/MultiSpec/Intro5–01.pdf, School of Electrical and Computer Engineering, Purdue University (accessed 10 March 2005).

LEE, C. and LANDGREBE, D.A., 1993, Feature extraction based on decision boundaries. *IEEE Transaction on Pattern Analysis and Machine Intelligence*, **15**, pp. 388–400.

LEWIS, M.M., 2001, Discriminating vegetation with hyperspectral imagery—What is possible? In *Proceedings of the Geoscience and Remote Sensing Symposium 2001 (IGARSS '01), IEEE 2001 International*, **6**, pp. 2899–2901.

OKI, K., LU, S., SARUWATARI, T., SUHAMA, T. and OMASA, K., in press, Evaluation of supervised classification algorithms for identifying crops using airborne-hyperspectral data. *International Journal of Remote Sensing*, **27**, pp. 1993–2002.

ORTIZ, M.J., FORMAGGIO, A.R. and EPIPHANIO, J.C.N., 1997, Classification of croplands through integration of remote sensing, GIS and historical database. *International Journal of Remote Sensing*, **18**, pp. 95–105.

SHAHSHAHANI, B.M. and LANDGREBE, D.A., 1994, The effect of unlabeled samples in reducing the small sample size problem and mitigating the Hughes phenomenon. *IEEE Transactions on Geoscience and Remote Sensing*, **32**, pp. 1087–1095.